



Immediate development of processing windows for selective electron beam melting using layerwise monitoring via backscattered electron detection

Christoph R. Pobel*, Christopher Arnold, Fuad Osmanlic, Zongwen Fu, Carolin Körner

University of Erlangen-Nuremberg, Department of Materials Science, Chair of Materials Science and Engineering for Metals (WTM), Martensstrasse 5, 91058 Erlangen, Germany

ARTICLE INFO

Article history:

Received 20 February 2019
Received in revised form 7 March 2019
Accepted 11 March 2019
Available online 16 March 2019

Keywords:

Additive manufacturing
Selective electron beam melting
Process monitoring
Backscattered electrons
Processing window
Ti-6Al-4V

ABSTRACT

The availability of a reliable processing window is the basic requirement for processing new materials via selective electron beam melting (SEBM). Typically, these processing windows are derived by a time-consuming procedure comprising fabrication, metallographic preparation and analysis of standardized specimens for every parameter set. This study demonstrates the immediate development of a processing window during one single SEBM process. An electron optical image acquisition system provides the necessary information for evaluation and subsequent adaption of process parameters. It is shown that this immediate approach delivers processing windows with sufficient accuracy, while the required time is substantially reduced from weeks or even months to several hours.

© 2019 Elsevier B.V. All rights reserved.

1. Introduction

Selective Electron Beam Melting (SEBM) is a powder bed-based Additive Manufacturing (AM) technology, which allows the near-net-shape fabrication of fully dense metallic components with complex geometries [1]. So far, numerous materials, e.g. Titanium alloys [2,3], pure Cu [4], stainless steel [5] and Ni-based superalloys [6], have been successfully processed using SEBM. In order to build dense parts with good surface quality and mechanical properties, reliable process parameters for each material have to be experimentally determined. For each parameter set within the processing map, standardized specimens have to be fabricated, cleaned from residual powder and metallographically prepared. Subsequently, the porosity of each specimen is determined by microscopic analysis [3]. This commonly used, time-consuming approach is necessary, because during SEBM the ambient conditions impede sufficient insight into the process. The elevated processing temperature and the high-vacuum atmosphere require the process to be conducted within a build chamber that provides only small viewports to the operator.

Pursuing the goal of enhancing insight into the process and thus improving control and quality, various tools for in-situ process

monitoring have been investigated [7]. It has been shown that layerwise acquisition of images via near-infrared thermography delivers information about porosity of the molten layer, which correlates with porosity inside the final sample [8,9]. Main difficulty of this approach is the evaporation of volatile alloy components from the melt pool that causes metallization on the camera observation window, which has to be counteracted by using mechanical shutters or spooling film systems [8,9]. Recently, Arnold et al. described an alternative approach of layerwise monitoring of the SEBM process by detecting backscattered electrons (BSE) to acquire electron optical (ELO) images in a way comparable to scanning electron microscopy (SEM) [10]. It has been shown that the resolution of the obtained images is sufficient to depict surface defects, and that these defects correlate with the porosity in the final specimen [10].

In this work, the process monitoring system and the findings presented by Arnold et al. [10] were applied to the development of processing windows. As an exemplary material Ti-6Al-4V was chosen, because it has been deeply studied for SEBM in former works [2,3]. After verification through comparison with the traditional approach, a new processing window for SEBM using different layer thickness was established based on the ELO observation.

* Corresponding author.

E-mail address: christoph.pobel@fau.de (C.R. Pobel).

2. Experimental

The SEBM processes took place on an in-house development SEBM system named ATHENE which is capable of recording ELO images during SEBM process. A more detailed description of the SEBM- and ELO-system can be found elsewhere [10]. The conventional SEBM process starts by applying a powder layer. Preheating with an unfocused electron beam ensures stable conditions for subsequent melting of a defined cross-section with a focused beam. After lowering the build platform by the thickness of one layer, the cycle is repeated until the three-dimensional components are completed. When applying the ELO approach, an additional image acquisition step was added after melting step. These ELO images were recorded using a beam current of 3 mA while spatial resolution and pixel exposure time were set to 34 $\mu\text{m}/\text{pixel}$ and 0.4 $\mu\text{s}/\text{pixel}$, respectively. The images were immediately displayed to the operator to classify the specimen surfaces as porous, good or uneven. In case of the conventional approach, the as-built

specimens were metallographically prepared and afterwards analyzed by optical microscopy.

For all experiments, plasma atomized Ti-6Al-4V powder (grade 23, particle size: 45–105 μm , Tekna Plasma Europe, Mâcon, France) was used. Cuboid specimens with a base area of 15 \times 15 mm^2 were fabricated. All cross-sections were molten using a snake hatch method [3] with a constant line spacing h_s of 100 μm . The hatch direction was rotated by 90° after each layer. The process was operated at a temperature between 730 and 750 °C and a controlled vacuum atmosphere of 0.3 Pa helium.

Two processing windows for Ti-6Al-4V were established by investigating different parameter sets of beam power P and scan speed v_s . First, a processing window for layer thickness $l_z = 50 \mu\text{m}$ was developed by fabricating a cuboid of 15 mm height for each parameter set and using the conventional method to determine the porosity and surface quality. To verify the capability of ELO imaging for process development, additional sets for $l_z = 50 \mu\text{m}$ were investigated using the ELO approach. Second, the processing window for $l_z = 100 \mu\text{m}$ was developed by solely applying the ELO approach. In this case, the height was kept constant at 2.5 mm for each parameter set, which corresponds to 50 layers for $l_z = 50 \mu\text{m}$ and 25 layers for $l_z = 100 \mu\text{m}$. This 2.5 mm build height for the surface quality analysis was an empirical value to account for transition effects between sections [10]. To evaluate the porosity and unevenness, the cross-sections of the molten layers between 1.5 mm and 2.5 mm in build height were analyzed. This approach was chosen, since no significant changes in the molten layer quality were detected after around 1.5 mm of build height using a certain parameter setup.

3. Results and discussion

Fig. 1 shows an exemplary ELO image of nine cuboid specimens. P and l_z were kept constant at 1000 W and 100 μm , respectively; while v_s was adjusted as indicated. By increasing v_s from 2.5 to 6.0 m/s, the molten layers show an improving quality from significantly uneven (2.5 m/s and 3.0 m/s) to completely plane surfaces. With further increased speeds from 7.0 to 10.0 m/s, porosity is observed due to the decreasing energy input at higher scan velocities. In case of the ELO approach, an analog classification was conducted for all parameter sets to derive the complete processing window.

Fig. 2a shows the processing window for $l_z = 50 \mu\text{m}$ and $h_s = 100 \mu\text{m}$. The data derived by the conventional approach were

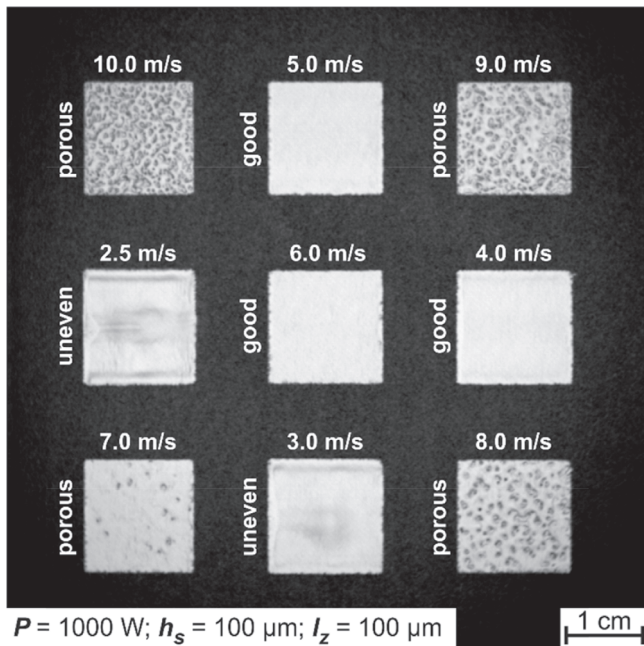


Fig. 1. Representative ELO image for processing window development ($l_z = 100 \mu\text{m}$; $h_s = 100 \mu\text{m}$; $P = 1000 \text{ W}$) with different v_s .

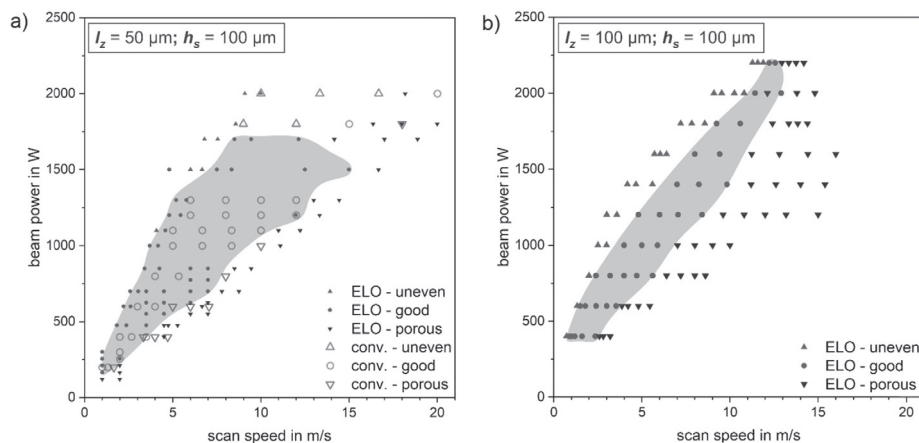


Fig. 2. Two processing windows generated on ATHENE. The green area represents an estimated stable process region for SEBM of dense samples with even surface. (a): Combination of conventional and ELO approaches ($h_s = 100 \mu\text{m}$; $l_z = 50 \mu\text{m}$); (b): Solely ELO approach for $h_s = 100 \mu\text{m}$, $l_z = 100 \mu\text{m}$. (For interpretation of the references to colour in this figure legend, the reader is referred to the web version of this article.)

based on 43 analyzed specimens, which required several build jobs. Meanwhile, 82 data points were obtained according to the evaluation of ELO images. The green area depicts the estimation of a stable processing region, where no uneven or porous samples are expected. When comparing both approaches, a good qualitative agreement can be stated. Especially the transition from porous to good samples at low v_s shows the conformity of results for both approaches.

Fig. 2b shows the processing window for $l_z = 100 \mu\text{m}$ and $h_s = 100 \mu\text{m}$, which was determined by solely following the ELO approach. During one single build job, it was possible to test 95 different parameter sets and determine a complete window over the course of merely 4 h, while the process development could take several weeks or even months when using the conventional method. This shows the vast potential of BSE detection for developing stable processes of new materials and powders. Especially the elimination of process environment variations between different processes increases the validity of the produced data. While the conventional approach limits the classification of porosity to a 2D-microsection, the ELO approach enables a quasi-3D evaluation of the specimen. By using the conventional approach, only one cross-section in the xz-plane was analyzed, while during ELO observation multiple 2D images of the molten layers in the xy-plane were gained and could be stacked upon each other to reconstruct a 3D density map of the sample [10].

When comparing the processing windows for $l_z = 50 \mu\text{m}$ and $l_z = 100 \mu\text{m}$, a narrower shape of the latter is evident. Due to the increase in volume that has to be molten when the layer thickness increases, the boundary between porous and good parameter sets is shifted to higher energy. The boundary between good and uneven specimens remains rather the same, because the energy input provoking an uncontrolled dynamic of the melt pool is unaffected by layer thickness.

4. Conclusion

During SEBM, layerwise monitoring via BSE detection was used for developing processing windows. The real time process monitoring enabled the evaluation of melting parameter sets during the actual SEBM process. In this work, two processing windows for different layer thicknesses were determined. Compared to the conventional approach, which required substantial effort, the ELO approach showed comparable results, and offered the possibility to achieve the development of a processing window within one

SEBM build process over the course of few hours instead of weeks to months. It was shown that the ELO approach greatly reduced the effort necessary to generate processing windows for different setups, making it highly viable for developing stable processing conditions for new powders and materials in SEBM.

Conflict of interest

None.

Acknowledgment

We gratefully thank the German Research Foundation (DFG) for funding our research in the Collaborative Research Centre SFB814, project B2.

References

- [1] L.E. Murr, S.M. Gaytan, D.A. Ramirez, E. Martinez, J. Hernandez, K.N. Amato, P. W. Shindo, F.R. Medina, R.B. Wicker, Metal fabrication by additive manufacturing using laser and electron beam melting technologies, *J. Mater. Sci. Technol.* 28 (1) (2012) 1–14.
- [2] N. Hrabe, T. Quinn, Effects of processing on microstructure and mechanical properties of a titanium alloy (Ti-6Al-4V) fabricated using electron beam melting (EBM), part 1: distance from build plate and part size, *Mater. Sci. Eng.: A* 573 (2013) 264–270.
- [3] C.R. Pobel, F. Osmanlic, M.A. Lodes, S. Wachter, C. Körner, Processing windows for Ti-6Al-4V fabricated by selective electron beam melting with improved beam focus and different scan line spacings, *Rapid Prototyping J.* (2018).
- [4] R. Guschlbauer, S. Momeni, F. Osmanlic, C. Körner, Process development of 99.95% pure copper processed via selective electron beam melting and its mechanical and physical properties, *Mater. Charact.* 143 (2018) 163–170.
- [5] Y. Zhong, L.-E. Rännar, L. Liu, A. Koptuyg, S. Wikman, J. Olsen, D. Cui, Z. Shen, Additive manufacturing of 316L stainless steel by electron beam melting for nuclear fusion applications, *J. Nucl. Mater.* 486 (2017) 234–245.
- [6] E. Chauvet, P. Kontis, E.A. Jäggle, B. Gault, D. Raabe, C. Tassin, J.-J. Blandin, R. Dendievel, B. Vayre, S. Abed, G. Martin, Hot cracking mechanism affecting a non-weldable Ni-based superalloy produced by selective electron beam melting, *Acta Mater.* 142 (2018) 82–94.
- [7] M. Grasso, B.M. Colosimo, Process defects and in situ monitoring methods in metal powder bed fusion: a review, *Meas. Sci. Technol.* 28 (4) (2017) 044005.
- [8] J. Schwerdtfeger, R.F. Singer, C. Körner, In situ flaw detection by IR-imaging during electron beam melting, *Rapid Prototyping J.* 18 (4) (2012) 259–263.
- [9] R.B. Dinwiddie, R.R. Dehoff, P.D. Lloyd, L.E. Lowe, J.B. Ulrich, Thermographic in-situ process monitoring of the electron-beam melting technology used in additive manufacturing, in: *Thermosense: Thermal Infrared Applications XXXV International Society for Optics and Photonics*, 2013, p. 87050K.
- [10] C. Arnold, C. Pobel, F. Osmanlic, C. Körner, Layerwise monitoring of electron beam melting via backscatter electron detection, *Rapid Prototyping J.* 24 (8) (2018) 1401–1406.